Structure by NMR of Antitumor Drugs Aclacinomycin A and B Complexed to d(CGTACG)†

Danzhou Yang and Andrew H.-J. Wang*

Biophysics Division and Department of Cell & Structural Biology, University of Illinois at Urbana-Champaign, Urbana, Illinois 61801

Received December 16, 1993; Revised Manuscript Received April 6, 1994®

ABSTRACT: Aclacinomycins A and B are anthracycline antibiotics with potent antitumor activity. Each consists of an alkavinone aglycon chromophore and a trisaccharide (rhodosamine–deoxyfucose–cinerulose A or B) tail attached at the C^7 of ring A of the alkavinone. The structures of the 2:1 aclacinomycin–d(CGTACG) complexes have been studied in solution by 2D NMR spectroscopy using nuclear Overhauser effect data. SPEDREF refinement procedure (incorporating simulated annealing within the program X-PLOR) was used to obtain an ensemble of refined structures which reveal that the elongated alkavinone is intercalated between the CpG steps and the trisaccharide lies in the minor groove. In the complex, the two GC Watson–Crick base pairs (C1:G12 and G2:C11) that wrap around the aglycon have large buckles, consistent with those seen in the crystal structures of other anthracycline–DNA complexes. The intercalation geometry of aclcainomycin is a hybrid between those of daunorubicin and nogalamycin. Ring D of alkavinone is sandwiched by the C1 and C11 bases. The deoxyfucose ring of the trisaccharide is close to the DNA backbone at the A4 nucleotide, forcing the DNA helix to kink toward the major groove (with the opening in the minor groove). The kink between two adjacent A–T base pairs (T3–A10 and A4–T9) causes the adenine $A4N^6$ to form two hydrogen bonds to $T9O^4$ (interstrand) and $T3O^4$ (intrastrand) simultaneously. There is a small unwinding of the helix resulting from the intercalated aclacinomycin. Several potential hydrogen bonds exist between the drug and the guanine bases in the minor groove of the helix. Multiple molecular species coexist in the solution of the 1:1 mixture of aclacinomycin and d(CGTACG) due to the slow rate of drug binding to DNA.

Anthracycline antibiotics constitute an important class of antitumor drugs. Most notable members include daunorubicin and doxorubicin, which are presently in widespread clinical use (Lown, 1988; Crooke & Reich, 1980). Many new antibiotics, natural or semisynthetic, have been searched and tested for better therapeutic properties, e.g., lower cardiotoxicity and/or lower induction of resistance to cancer cells. Previous studies showed that the anthracycline family of antibiotics are DNA intercalators and that their DNA binding affinity and sequence specificity are likely related to their biological activities (Wang, 1992). A detailed understanding of the drug–DNA interactions at the molecular level is the first step toward the design of potentially useful and better agents (Denny, 1989).

Aclacinomycins A and B (Figure 1) are members of the anthracycline family of antibiotics with potent anticancer activity (Oki et al., 1981). Aclacinomycin A has been used in combination with doxorubicin to enhance the effectiveness of doxorubicin toward cancer cells which have acquired drug resistance (Millot et al., 1989; Tapiero et al., 1988). Aclacinomycin A has an antagonistic effect on DNA cleavage by topoisomerase II stimulated by daunorubicin (Jensen et al., 1991).

These two new anthracyclines contain a trisaccharide moiety attached to the C^7 position of the ring A of the aglycon chromophore alkavinone. Their aglycon rings are similar to those of daunorubicin and nogalamycin in that the alkavinone has three unusubstituted C–H positions in ring D and an O^9 hydroxyl group in ring A, as in daunorubicin. But they also

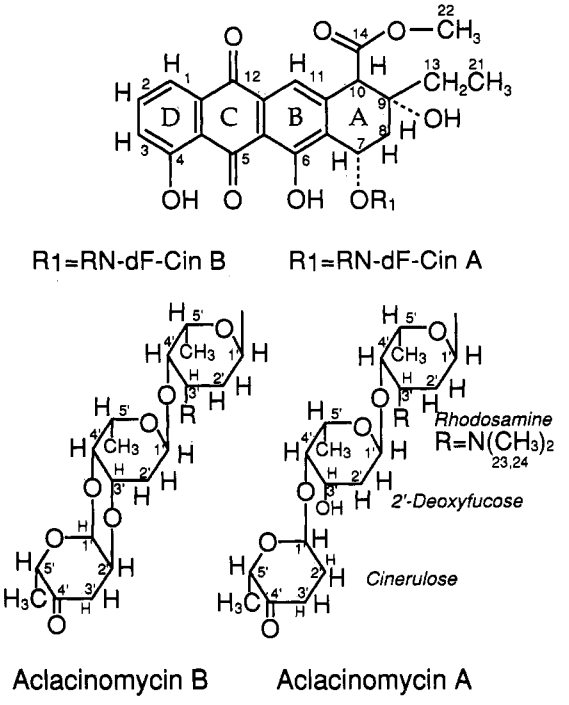

FIGURE 1: Molecular formulas of the aclacinomycins A and B with the numbering system used in this paper. The molecules contain an aglycon chromophore (alkavinone, abbreviated AKN) with four fused rings (A–D). A trisaccharide is attached to the aglycon at the C^7 position. The sugars of the trisaccharide are L-rhodosamine (RN), 2′-deoxy-L-fucose (dF), and cinerulose A or B (CinA or CinB).

† This work was supported by NIH Grants CA-52506 and GM-41612 to A.H.-J.W. The Varian VXR500 spectrometer was supported by NIH shared instrumentation grant 1S10RR06243.

* To whom correspondence should be addressed.

® Abstract published in *Advance ACS Abstracts,* May 15, 1994.

0006-2960/94/0433-6595$04.50/0

have an open H^{11} position in ring B and a carbomethoxy group at C^{10} position, as in nogalamycin. Other related antibiotics include betaclamycins A and B, which have identical trisaccharides but with a different aglycon β-rhodomycinone (Yoshimoto et al., 1992).

Even though aclacinomycin is expected to intercalate DNA, the molecular details of its binding mode are unknown. The issue of its nucleotide sequence specificity has been addressed only in a preliminary manner (DuVerney et al., 1979). This is in contrast to other anthracyclines, such as daunorubicin (Chaires et al., 1987) or nogalamycin (Fox & Alam, 1992), which have been more extensively studied.

X-ray crystallography and NMR spectroscopy are two powerful methods which provide insight into the anthracycline drug binding to DNA at the molecular level [reviewed in Wang (1992), Leonard et al. (1993), and Zhang et al. (1993)]. In particular, the use of a combination of NOE-based distance constraints and molecular dynamics refinement has been shown to be extremely valuable in determining the solution structure of biomolecules (Gilbert & Feigon, 1991). Relevant examples include the studies of the 2:1 nogalamycin–d(TGCATGCA) complex (Zhang & Patel, 1990) and the 1:1 nogalamycin–d(GACGTC) complex (Searle & Bicknell, 1992). Here we analyzed the binding of aclacinomycins A and B to the DNA hexamer d(CGTACG) by a quantitative treatment of the NOE data. Our goal is to understand the molecular basis of aclacinomycin–DNA interactions in solution. Such information may be useful in correlating the anticancer activity of aclacinomycins with their structures.

MATERIALS AND METHODS

The oligonucleotide hexamer DNA d(CGTACG), or CGTACG for short, was synthesized on a DNA synthesizer. Aclacinomcyin A (AclaA) was obtained from the National Cancer Institute, and aclacinomycin B (AclaB) was a gift from Dr. Osamus Johdo of Mercian Co. (Fujisawa, Japan). We have analyzed these two drugs in aqueous solution by 1D and 2D NMR spectroscopy and found that both samples contained some impurities (<10%) whose identities were not determined. The resonances of those impurities have separate chemical shifts, and they do not have significant nuclear Overhauser effect crosspeaks between them and those from aclacinomycin or DNA in the complex. Consequently, we concluded that those impurities should not affect the structural analysis, and the samples were used without further purification.

For the studies of drug–DNA complexes, drug molecules were dissolved in methanol as stock solutions. The solutions of aclacinomycin–CGTACG complexes for NMR studies were prepared by dissolving the ammonium salt of the DNA hexamer plus the appropriate amounts of aclacinomycin stock solution in 0.50 mL of phosphate buffer solution (50 mM sodium phosphate, pH 7.0, 150 mM NaCl in 99.8% D_2O) to produce a final concentration of 4 mM duplex. The solution was lyophilized twice with 99.8% D_2O and then dried in an NMR tube with a stream of argon gas, and finally 0.50 mL of 99.96% D_2O was added to produce the sample.

Both 1D and 2D NMR spectra were recorded on either a GE GN500 or a Varian VXR500 500-MHz spectrometer. The chemical shifts (in ppm) are referenced to the HDO peak, which is calibrated to 2,2-dimethyl-2-silapentane-5-sulfonate (DSS) at different temperatures. Magnitude COSY and phase-sensitive NOESY spectra were recorded as 512 t_1 blocks of 2048 complex points each (in the t_2 dimension) and averaged for 16 scans per block during the recycle delay of 1.0 s for the COSY and 4.0 s for the NOESY. The mixing time for the NOESY experiments was 100 ms. The 2D data sets were processed with the program FELIX v.1.1 (Hare Research, Woodinville, WA) using Silicon Graphics workstations. For the 2D data sets, the 2048 complex points in the t_2 dimension were apodized with a 60°-shifted sine-bell squared function (skew factor of 1.2). The 512 complex points in the t_1 dimension were apodized similarly and zero-filled to 2048 points prior to the Fourier transform.

The structure refinement of the 2:1 complex has been carried out by the procedure SPEDREF (Robinson & Wang, 1992), except that the conjugated gradient minimization process has been replaced by simulated annealing. Our approach utilizes all relevant NOE crosspeaks (excluding those from the impurities). The mixing time of 100 ms was selected as it gives an optimum number of NOE observables without the problem of severe spin diffusion or yielding too few NOEs. The recovery inversion experiment was used to determine the approximate T_1 relaxation time for every spin, with the average T_1 of 1.6 s for all protons. The recycle time of 4.0 s is more than 2 times the average T_1, amounting to about 90% complete recovery on average. The correlation time τ_c was estimated to be about 9.5 ns for the 2:1 complexes. For comparison, the free DNA CGATCG duplex at 2.4 mM concentration has a τ_c of 4.0 ns, determined by the procedure described before (Robinson & Wang, 1992).

The force field constants of DNA are taken from X-PLOR (Brunger, 1992). The aclacinomycins A and B were constructed using QUANTA (Polygen, Waltham, MA). The alkavinone (AKN) aglycon was created starting with the daunomycinone (DAN) aglycon of daunorubicin. Standard atom types in the QUANTA package were used for the necessary chemical modifications in going from DAN to AKN. The partial charges for the alkavinone were calculated using the semiempirical AM1 Hamiltonian of the AMPAC program described earlier (Sriram et al., 1991). The sugars were generated using daunosamine as a starting framework and modified appropriately by QUANTA. The trisaccharide moiety of aclacinomycin A was pieced together from rhodosamine (RN), 2-deoxyfucose (dF), and cinerulose A (CinA), whereas the trisaccharide moiety of aclacinomycin B was made by joining rhodosamine and the fused dF–CinB tricyclic moiety, whose atomic coordinates were from the crystal structure (Richle et al., 1972). Both trisaccharides were then subjected to energy minimization using the method of steepest descent, and their partial charges were obtained from the representative fragments available in QUANTA.

Molecular dynamics (MD) simulation and simulated annealing (SA) were carried out using the program X-PLOR (Brunger, 1992). The SA was carried out by performing molecular dynamics at 1000 K for 100 ps initially. Models along the trajectory were selected every 10 ps, and they were slowly cooled by 25 deg every 250 fs to a temperature of 300 K with NOE constraints. It was found that the deviations among the models after 40 ps of SA were very small. Subsequently, 40 ps of SA was considered to be sufficient. A starting model, constructed as described later, was subjected to this SA refinement procedure using the data set of NOE constraints obtained by the program SPEDREF (Robinson & Wang, 1992). At the end of each 40-ps SA refinement cycle, the calculated NOE spectrum of the resulting model was compared with the experimental NOE spectrum to produce a new data set of NOE constraints, which became the NOE input of the next 40-ps SA refinement cycle. This

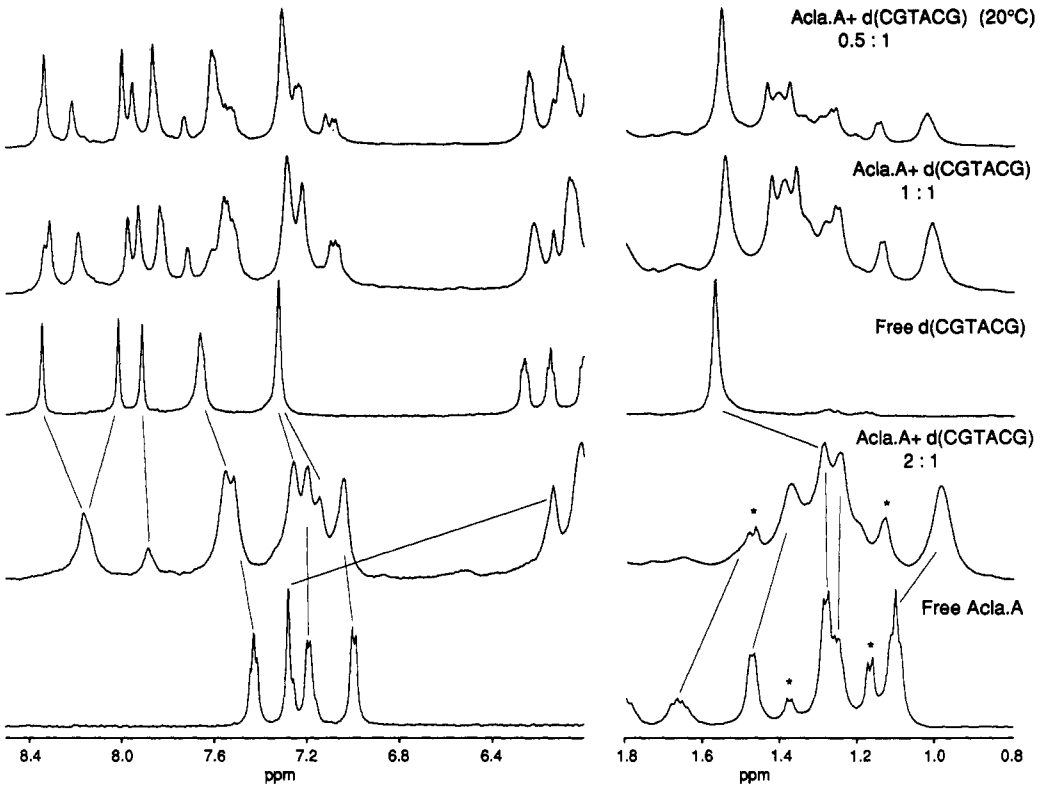

FIGURE 2: One-dimensional ^{1}H NMR spectra of the aromatic and methyl regions of the free DNA, 0.5:1, 1:1, and 2:1 aclacinomycin A–d(CGTACG) complexes, and free aclacinomycin A. The spectra were recorded at 25 °C, except that of the 0.5:1 complex, which was recorded at 20 °C. Resonances marked with asterisks are from the impurity of the drug sample.

process was iterated 20 times, at which point a convergence of the NMR R-factor (defined as $\sum|N_o - N_c|/\sum N_o$, where N_o and N_c are observed and simulated NOEs, respectively) was achieved. This procedure ensured that a wider range of conformational space was searched, in comparison with the procedure using conjugated gradient minimization.

The definition and nomenclature of the torsion angles and conformational parameters (e.g., helical twist angles, base pair buckles) of DNA follow the convention adopted by the Cambridge Workshop (Dickerson et al., 1989).

RESULTS AND DISCUSSION

1D Spectra. We have titrated aclacinomycin A with CGTACG at different ratios. The 1D NMR spectra in Figure 2 show that the free aclacinomycin A and free DNA have sharp resonances. When the ratios of AclA to CGTACG are 0.5:1 and 1:1, the spectra show complex patterns. However, when the ratio reaches 2:1, the spectra become considerably simplified, showing that a stable and symmetric 2:1 complex is formed. All nonexchangeable resonances of the free DNA and free drugs (AclaA and AclaB) have been unambiguously assigned by 2D NOESY using the procedure described later.

The temperature-dependent profiles of the one-dimensional ^{1}H NMR spectra of the aromatic and methyl regions of the 2:1 AclaA–CGTACG complexes are shown in Figure 1S (supplementary material). The chemical shifts of most of the resonances vary slightly on raising the temperature from 5 °C to 55 °C (Figure 1S). The resonances are broad for spectra recorded below 25 °C, suggesting that the binding dynamic of the drug is in the intermediate-to-slow exchange rate range. Precipitate began to appear in the solution of the complex under low temperature (<25 °C), and the precipitate did not redissolve completely. Consequently, all 2D NOESY spectra were recorded at temperatures higher than 25 °C.

Resonances of the drug protons in the complex show different temperature-dependent line shape/line width profiles (Figure 1S), which suggests that the motional property of the complex has variable effects on those protons. Note that the KH^2 and KH^3 resonances gradually sharpen in going from 5 °C to 55 °C, whereas the KH^{11} becomes sharp at 35 °C but extremely broad at 55 °C. This observation reflects the different environment of those alkavinone protons. KH^{11} is completely buried in the intercalation cavity; thus it is under the strong ring current effect from the aromatic bases of DNA. This has resulted in a large upfield chemical shift of 1.18 ppm for KH^{11} in going from the free form to the bound form (Figure 2). Upon the temperature being raised, the rate of exchange of KH^{11} between the free and bound forms became comparable to its resonance frequency difference (~600 Hz) at 55 °C, as manifested by the broad resonance of KH^{11}. This observation also shows that a considerable population of the bound drug remains at 55 °C.

Resonance Assignment. Several 2D NOESY spectra of the 2:1 complexes were collected, which included the AclaA–CGTACG at 25 °C and 40 °C and the AclaB–CGTACG at 30 °C and 40 °C. The complete experimental 2D NOESY spectrum of the AclaB–CGTACG complex at 30 °C is shown in Figure 2S. Numerous NOE crosspeaks are observed, indicating a well-defined structure of the complex. In this work, the results obtained from the AclaA–CGTACG and AclaB–CGTACG complexes are very similar. Therefore, only the results from the latter complex are used for discussion unless otherwise stated.

The assignment of the resonances of the complex was established by starting with the aromatic–H$^{1'}$ fingerprint region using the sequential assignment strategy analogous to that used previously for the 2:1 nogalamycin–CGTACG complex (Robinson et al., 1990). Figure 3 shows the expanded region

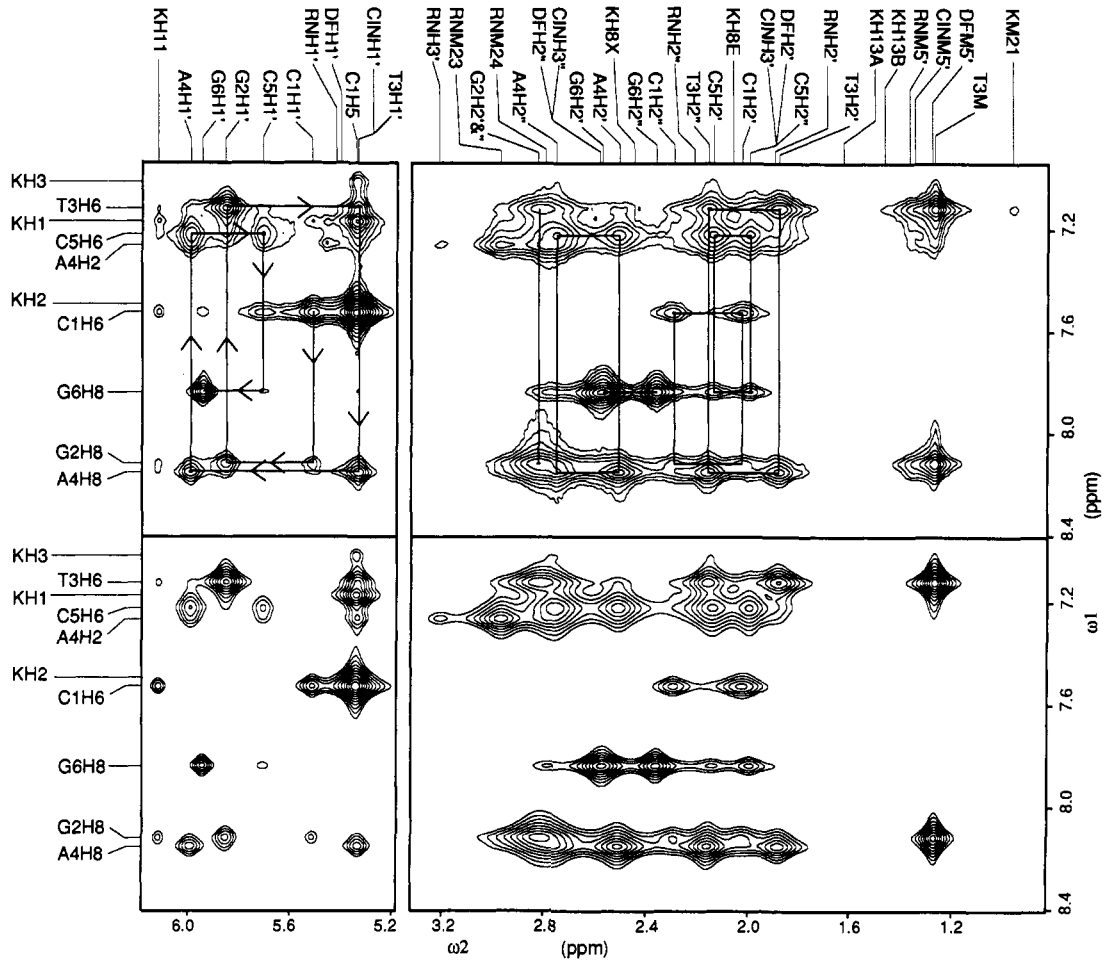

FIGURE 3: Expanded regions of the 2D NOESY spectra (top panels, experimental; bottom panels, simulated from the refined model) which provided key information in the assignments of resonances. Left panels show crosspeaks between the aromatic protons (7.0–8.4 ppm) and the $H^{1'}$ protons. The sequential assignment pathway is indicated. Right panels show crosspeaks between the aromatic protons and the $H^{2'},H^{2''}$ protons. Each aromatic proton has crosspeaks to its own $H^{2'}/H^{2''}$ as well as to those from the preceding (5′-side) nucleotide which are connected by a rectangular box.

consisting of the aromatic-to-$H^{1'}$ and aromatic-to-$H^{2'}/H^{2''}$ crosspeaks. The sequential connectivity of the aromatic-to-$H^{1'}$ pathway can be traced without interruption. However, it is clear that the intensities between the $C1H^{1'}$–$G2H^8$ and the $C5H^{1'}$–$G6H^8$ crosspeaks are significantly weaker than those of the other internucleotide (i.e., $G2H^{1'}$–$T3H^6$, $T3H^{1'}$–$A4H^8$, and $A4H^{1'}$–$C5H^6$) crosspeaks. This suggests that the dinucleotide C1pG2 and C5pG6 steps are distorted and no longer have the normal B-DNA backbone conformation. (A step is defined as the environment associated with two adjacent bases in a dinucleotide). The aromatic-to-$H^{2'}/H^{2''}$ crosspeaks possess the same intensity pattern. Note that the $G2H^8$–$C1H^{2'}/H^{2''}$ and $G6H^8$–$C5H^{2'}/H^{2''}$ crosspeaks are significantly weaker than the remaining corresponding crosspeaks. The aromatic–aromatic crosspeaks, shown in Figure 4, also support the contention that the C1pG2 and C5pG6 steps are distorted. For example, the $C1H^6$–$G2H^8$ and $C5H^6$–$G6H^8$ crosspeaks are absent, indicating that the normal stacking interactions in free B-DNA (Figure 4B) are gone.

Taking those data together, we concluded that the 2:1 complex has its intercalation sites at the C1pG2 and C5pG6 steps. The next question was, How do the aclacinomycins bind at those intercalation cavities? To answer this, we needed to have a complete assignment of all the protons. In Figure 4A, there are three very strong, still unassigned NOE crosspeaks, and they must be from the aroamtic alkavinone H^1, H^2, and H^3 protons. Their identification could be made in a straightforward manner.

The correct assignments of the aromatic (of DNA and drug), $H^{1'}$, and $H^{2'}/H^{2''}$ resonances allowed the assignments to be extended to other regions. In the end, all resonances have been assigned, and their chemical shifts are tabulated in Table 1. The largest changes in chemical shift between the free and the bound forms are associated with the alkavinone KH^{11} ($\Delta\delta$ = +1.18 ppm) and the $C1H^5$ ($\Delta\delta$ = +0.58 ppm) and $C5H^5$ ($\Delta\delta$ = –0.57 ppm) protons. These data support the idea that the alkavinone is sandwiched between the two cytosines so that the ring current effects have mutually affected their chemical shifts.

Model of the Complexes. The construction of a starting model of the complex requires additional distance constraint information in order to place the drug in the intercalation cavity as accurately as possible. Figure 5 shows the 1D slices through the resonances of the alkavinone proton (H^1, H^2, H^3, and H^{11}) of the 2D NOESY spectrum of the 2:1 AclaB–CGTACG complex. The NOE intensities seem to show that KH^1 is close to both $C1H^5$ and $C5H^5$, KH^2 is closer to $C1H^5$, and finally KH^3 is closer to $C5H^5$. However, due to the overlaps of certain resonances, the apparent intensities of the KH^1-to-$C5H^5$ and the KH^2-to-$C1H^5$ crosspeaks in Figure 5 are not their true values.

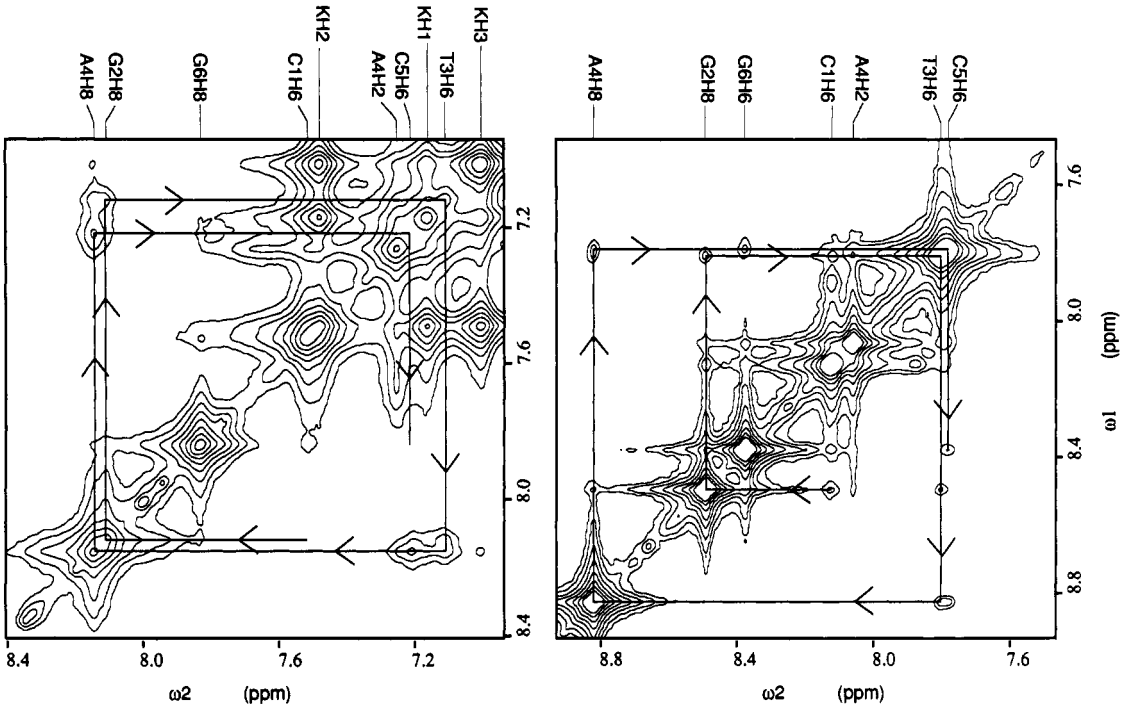

FIGURE 4: Expanded aromatic–aromatic region of the experimental 2D NOESY spectra. The internucleotide connectivity pathway is indicated. (A, left) The 2:1 complex of AclaB–d(CGTACG) at 30 °C. (B, right) Free d(CGTACG) at 5 °C.

Table 1: ^{1}H NMR Chemical Shifts (ppm) of DNA and Drug at 30 °C

Nonexchangeable Proton Chemical Shifts of Free and Bound d(CGTACG)

		H8/6	H5,H2,Me	H1′	H2′	H2″	H3′	H4′	H5′	H5″
C1	f-DNA	7.65	5.92	5.80	2.03	2.43	4.70	4.04		
	b-DNA	7.52	5.34	5.51	2.03	2.30	4.48	4.31	3.64	3.79
	Δ	0.13	***0.58***	0.29	0.00	0.13	0.22	–0.27		
G2	f-DNA	8.01		6.00	2.73	2.81	5.00	4.39		
	b-DNA	8.11		5.85	2.82	2.82	5.03	4.43	3.97	4.08
	Δ	–0.10		0.15	–0.09	–0.01	–0.03	–0.04		
T3	f-DNA	7.32	1.57	5.70	2.13	2.45	4.90	4.20?		
	b-DNA	7.11	1.27	5.33	1.88	2.16	4.75	4.09	4.13	4.09
	Δ	0.21	0.30	***0.37***	0.25	0.29	0.15	0.11		
A4	f-DNA	8.34	7.66	6.26	2.74	2.88	5.05	4.45		
	b-DNA	8.15	7.26	5.99	2.51	2.75	4.95	4.30	3.90	4.10
	Δ	0.19	***0.40***	0.27	0.23	0.13	0.10	0.15		
C5	f-DNA	7.32	5.42	5.70	1.88	2.31	4.80	4.18		
	b-DNA	7.21	5.99	5.71	2.14	2.00	4.82	4.17	4.05	4.05
	Δ	0.11	***–0.57***	–0.01	–0.26	0.31	–0.02	0.01		
G6	f-DNA	7.91		6.14	2.60	2.38	4.67	4.18		
	b-DNA	7.83		5.95	2.58	2.36	4.62	4.07	3.86	4.01
	Δ	0.08		0.19	0.02	0.02	0.05	0.11		

Nonexchangeable Proton Chemical Shifts of Free and Bound Aclacinomycin B

	H1	H2	H3	H11	H10	H7	H8X	H8E	H13A	H13B	M21	M22
						Alkavinone						
f-drug	7.24	7.41	6.97	7.30	4.13	5.01	2.61	2.15	1.77	1.63	1.08	3.82
b-drug	7.17	7.48	7.01	6.12	4.21	4.85	2.45	2.06	1.63	1.46	0.97	3.58
Δ	0.07	–0.07	–0.04	***1.18***	–0.08	0.16	0.16	0.09	0.14	0.17	0.11	0.24

	H1′	H2′	H2″	H3′	H3″	H4′	H5′	MH5′	M23	M24
					Rhodosamine					
f-drug	5.51	2.15	2.30	3.68		4.40	4.27	1.46	2.99	2.99
b-drug	5.43	1.91	2.23	3.21		4.01	4.28	1.37	2.97	2.80
Δ	0.08	0.24	0.07	***0.47***		***0.39***	–0.01	0.09	0.02	0.19
					2′-Deoxyfucose					
f-drug	5.49	2.08	2.64	4.40		4.25	4.27	1.27		
b-drug	5.40	1.99	2.58	4.37		4.22	4.37	1.28		
Δ	0.09	0.09	0.06	0.03		0.03	–0.10	–0.01		
					Cinerulose B					
f-drug	5.38	4.62		2.08	2.64		4.91	1.37		
b-drug	5.33	4.57		2.00	2.58		4.95	1.35		
Δ	0.05	0.05		0.08	0.06		–0.04	0.02		

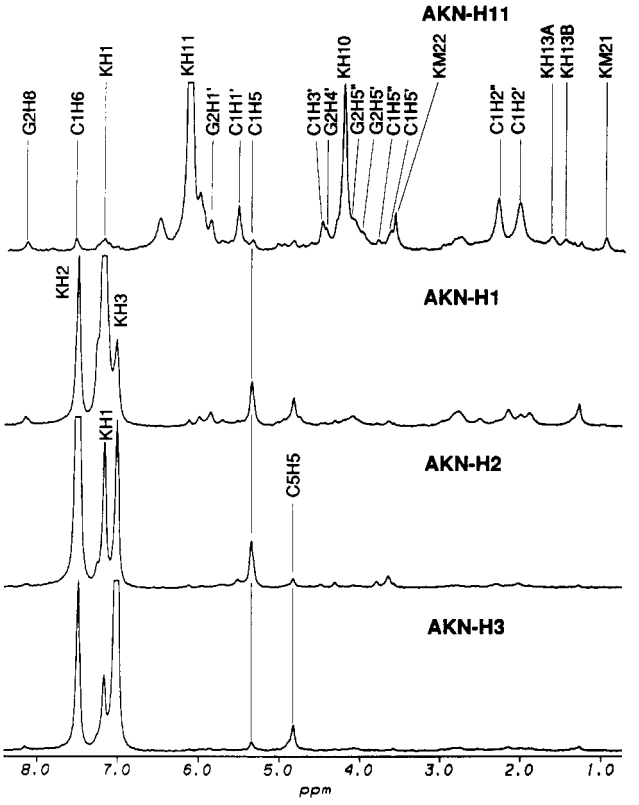

FIGURE 5: 1D slices through the 2D NOESY spectra of the 2:1 complex associated with four aclacinomycin B protons, AKN-H^1, -H^2, -H^3, and -H^{11}.

Careful inspection of the 2D NOESY spectra (Figures 3 and 4) revealed that the KH^1 and KH^3 protons, respectively, are spatially very close to $C1H^5$ and $C5H^5$ (both pairs having very strong nonoverlapping NOE crosspeaks), whereas KH^2 is spatially close to both $C1H^5$ and $C5H^5$. But the last two proton pairs are farther apart than those of KH^1 to $C1H^5$ and KH^3 to $C5H^5$. This suggests that ring D of AKN is sandwiched between C1 and C5. The position of the AKN aglycon ring is further defined by the NOE crosspeaks between the KH^{11} proton and many DNA protons, in particular those from the C1 and G2 residues. This clearly indicates that the AKN chromophore is oriented such that the ring edge containing H^{11} is facing toward the backbone of C1pG2. The correctness of the model is further reinforced by the 1D NOE slices through the H^7 and H^{10} resonances (data not shown).

To prepare a starting model for the NOE-restrained refinement, we considered the available crystal structures of two anthracycline–DNA complexes, the 2:1 complexes of daunorubicin–CGTACG (Wang et al., 1987) and nogalamycin–CGTACG (Liaw et al., 1989; Gao et al., 1990; Williams et al., 1990). In both complexes, the aglycon is intercalated in the CpG step but with a different position and orientation of the elongated AKN ring relative to the surrounding base pairs. Daunorubicin has its ring D protruding into the major groove side. Nogalamycin, in contrast, has its ring D stacked between the two neighboring base pairs. Since ring A of aclacinomycin has a carbomethoxy group at the C^{10} position, the AKN chromophore could not be in a position like that of the daunorubicin complex. An additional carbomethoxy group at the C^{10} position in the daunorubicin complex would create a severe clash between the carbomethoxy group and the C1:G12 base pair. Therefore, the initial model of the 2:1 AclaB–CGTACG complex has its aglycon sliding toward the minor groove relative to that in the daunorubicin complex but maintaining its orientation of the long vector of the aglycon (i.e., no twisting) in the intercalation activity.

Structure Refinements. For the structural refinement, we have assigned all NOE crosspeaks (except some associated with $H^{5'}/H^{5''}$ protons) and measured their integrals. The ambiguity due to those overlapping prochiral $H^{5'}/H^{5''}$ resonances does not seriously affect the refinement outcome, as the crosspeak intensities associated with $H^{5'}$ or $H^{5''}$ do not vary much regardless of whether a resonance is assigned as $H^{5'}$ or $H^{5''}$. There are 86 unique resonances (52 from DNA and 34 from aclacinomycin) and therefore 3612 total possible crosspeaks. We have measured 1879 NOEs (with proper line width/line shape by the program MYLOR) which were considered to be above the noise level, and they are used in the refinement. Although many of those crosspeaks are overlapped, the individual NOE peak integrals could be extracted by the deconvolution algorithm in the SPEDREF procedure (Robinson & Wang, 1992). It should be stressed that there is a degradation in the reliability of the measured NOE integrals proportional to the degree of overlaps. The more serious the overlap is, the less reliable the individual NOE intensity is.

The NMR *R*-factor based on this starting model is 36%. The analysis of the residual errors for each spin indicated that large discrepancies in the observed and calculated NOEs occurred with protons associated with the trisaccharide of aclacinomycin (especially the methyl groups), the 5'-end ($H^{5'}$, $H^{5''}$, and $H^{4'}$) of C1, and finally the G6 protons (Figure 3S). Twenty cycles of SPEDREF refinements (incorporating a simulated annealing step in each cycle) were carried out on the starting model. The refinements converged to *R*-factors in the range of 18.2–21% in the final 10 cycles. In this refinement, the entire model was kept with a twofold symmetry since the NMR spectra indicated a single resonance for every proton, even though there are two CGTACG strands and two aclacinomycins in the complex. The residual errors for each spin in the refined model are uniformly lower (Figure 3S). The methyl groups tend to have higher residual errors, which could be due to their inherent motional property or the anisotropic C–H angular orientation (relative to other protons) of the methyl groups.

The agreement between the experimental and calculated NOE integrals is shown in Figures 3 and 2S. To illustrate the good fit, we tabulate the respective values of the 50 largest observed and calculated NOEs between the drug and DNA protons (out of a total of 607 observed NOEs) (Table 2).

Structure of the Complex. An ensemble of the 10 refined structures of the 2:1 AclaB–CGTACG complex obtained from the fianl 10 SPEDREF-SA refinement cycles is shown in Figure 6. The largest root-mean-square deviation (rmsd) among these 10 structures is about 0.7 Å. Some parts of the complex have higher deviations, which may be due either to their motions or to the lack of NOEs. The G6 residue has the largest deviation. This is probably associated with the fraying of the terminal base pairs. The AKN aglycon is intercalated in the CpG step with a small rmsd, indicating a well-defined binding conformation. The cinerulose B has a large deviation, which more likely is due to the sparse number of NOE crosspeaks between protons from CinB and other protons.

A conspicuous feature of the refined model is the large buckle of the two GC base pairs (C1:G12 and G2:C11) that wrap around the aglycon. This is similar to those seen in the crystal structure of other anthracycline–DNA complexes (Wang, 1992). There are several possible hydrogen bonds between AclaB and DNA. The O^9 and O^7 atoms, both in the

Table 2: Experimental (N_o) and Calculated (N_c) NOE Crosspeak Intensities between Aclacinomycin B and DNA Protons

DNA	aclacinomycin B	N_o	N_c
Cyt1 H2′	Acl14 KH11	593	650
Cyt1 H2″	Acl14 KH11	582	770
Cyt1 H2″	Acl14 KH10	329	309
Cyt1 H1′	Acl14 KH11	308	339
Cyt1 H1′	Acl14 KM22	165	390
Cyt1 H5	Acl14 KH1	500	594
Cyt1 H5	Acl14 KH2	208	175
Cyt1 H6	Acl14 KH1	512	450
Gua2 H5′	Acl14 KH10	161	143
Gua2 H5′	Acl14 KM22	227	192
Gua2 H4′	Acl14 KH10	218	279
Gua2 H4′	Acl14 KH13A	431	600
Gua2 H4′	Acl14 KH13B	410	496
Gua2 H1′	Acl14 KH11	179	257
Gua2 H1′	Acl14 KH10	528	615
Gua2 H1′	Acl14 KH13A	246	232
Thy3 H5′	Acl14 KH10	164	132
Thy3 H5′	Acl14 KM21	360	327
Thy3 H5′	Acl14 KH13A	316	346
Thy3 H5″	Acl14 KM21	292	244
Thy3 H4′	Acl14 KM21	231	194
Thy3 H4′	Acl14 KH13A	138	152
Thy3 H4′	Acl14 RNH5′	245	214
Thy3 H1′	Acl14 RNH3′	121	161
Thy3 H1′	Acl14 RNH4′	88	107
Thy3 H1′	Acl14 RNH5′	129	129
Ade4 H5′	Acl14 RNH4′	208	217
Ade4 H5′	Acl14 DFH1′	225	256
Ade4 H5″	Acl14 DFH1′	175	195
Ade4 H4′	Acl14 RNM23	54	32
Ade4 H4′	Acl14 RNH4′	237	209
Ade4 H4′	Acl14 DFH1′	286	310
Ade4 H4′	Acl14 DFM5′	115	96
Ade4 H1′	Acl14 RNM23	94	88
Ade4 H2	Acl13 RNM23	164	384
Cyt5 H5′	Acl14 DFM5′	170	200
Cyt5 H4′	Acl13 RNM24	237	315
Cyt5 H1′	Acl13 RNH2′	334	261
Cyt5 H5	Acl13 KH3	305	347
Cyt5 H6	Acl13 KH3	138	96
Gua6 H5′	Acl13 RNH2′	260	264
Gua6 H5′	Acl13 RNH2″	269	328
Gua6 H5″	Acl13 RNH2″	252	294
Gua6 H4′	Acl13 RNH1′	394	466
Gua6 H4′	Acl13 RNH2′	641	662
Gua6 H4′	Acl13 RNH2″	794	938
Gua6 H1′	Acl13 KH7	342	409
Gua6 H1′	Acl13 RNH1′	437	577
Gua6 H1′	Acl13 RNH2″	226	205

axial positions, are 3.44 and 2.99 Å, respectively, from the N^2 of G2. The O^9 atom is 3.18 Å from the N^3 of G2. In addition, the O^{14} keto oxygen of the carbomethoxy group (at C^{10}) is 2.71 Å from the N^2 of G12.

The trisaccharide lies in the minor groove. The first sugar coming off the alkavinone, the rhodosamine ring, covers the G2:C11 base pair in the minor groove. The N-methyl groups ($N^{3'}$Me1 and $N^{3'}$Me2) are proximal to the A10-H^2, -$H^{1'}$, and -$H^{4'}$ and the C11–$H^{1'}$, -$H^{4'}$, and -$H^{5',5''}$ protons, consistent with the observed NOEs (Figure 2S and Table 2). Similarly the RN-$H^{3'}$ proton has a significant NOE to the A10-H^2 proton.

There are only a few definitive NOE crosspeaks between the dF and CinB (or CinA) sugar rings and DNA. Nevertheless, the rigidity of those sugars, especially the fused dF–CinB disaccharide, makes it possible to define the conformation of the trisaccharide tail. Several strong intratrisaccharide NOEs are clearly visible (data not shown). For example, the strong observed NOE crosspeaks between (1) the rhodosamine methyl group at the $C^{5'}$ position (RN-Me) and the $H^{1'}$ of the dF sugar (4.0 Å) and (2) the two rhodosamine N-methyl groups at the $C^{3'}$ position and the $C^{5'}$ methyl of the dF sugar (5.7 and 5.1 Å) define the glycosyl torsion angle between the rhodosamine and deoxyfucose. Since the dF–CinB disaccharide is a fused tricyclic moiety, the entire trisaccharide conformation is now defined. The refined structure puts the $H^{1'}$ proton of dF close to the $H^{4'}$ and $H^{5',5''}$ protons of the A4 residue. The observed NOEs, though somewhat overlapped in this region, are consistent with this structure (Table 2).

Table 1S lists the conformational parameters of the DNA double helix. A surprising feature of the structure is that the DNA duplex is clearly kinked (20°) at the T3pA4 step. This is due to the close contacts between the deoxyfucose sugar of AclaB and the A4 deoxyribose of DNA, which force the A4 nucleotide to open up in the minor groove side. Since there are two aclacinomycin B molecules in the symmetric complex, the interactions resulting from both AclaB molecules may reinforce each other's role in the deformation of the helix.

We have recently determined the crystal structure of a semisynthetic daunorubicin derivative MAR70, which has a disaccharide (daunosamine–deoxyfucose, or DN–dF) complexed to CGTACG (Gao et al., 1991). In this structure, no kinking of the helix in DNA was observed. The conformation of the disaccharide in MAR70 is not very different from that of aclacinomycin. The glycosyl torsion angles of (DN)$C^{3'}$–(DN)$C^{4'}$–(DN)$O^{4'}$–(dF)$C^{1'}$ and (DN)$C^{4'}$–(DN)$O^{4'}$–(dF)$C^{1'}$–(dF)$C^{2'}$ in the MAR70–CGTACG complex are 147° and 160°, respectively, whereas the corresponding angles in aclacinomycin B for (RN)$C^{3'}$–(RN)$C^{4'}$–(RN)$O^{4'}$–(dF)$C^{1'}$ and (RN)$C^{4'}$–(RN)$O^{4'}$–(dF)$C^{1'}$–(dF)$C^{2'}$ are both near 140°. We conclude that the kink in DNA is induced by the positioning of the AKN aglycon in the intercalation cavity, which resulted in a clash between the deoxyfucose and the A4 sugar.

Figure 7 shows in detail the intercalation geometry of aclacinomycin in the CpG step. As mentioned earlier, the overall position of the AKN ring is different from that of DAN ring, with the ring D of AKN moving toward the minor groove direction by about 1.2 Å [for comparison, see Wang et al. (1987) and Liaw et al. (1989)]. This creates a crowding between the drug sugar (dF ring) and the A4 deoxyribose, the reason for the DNA kinking at the TpA step.

Comparison of Free and Bound Aclacinomycins. When aclacinomycin is bound to DNA, it changes the conformation of the DNA double helix substantially. This is not surprising, because aclacinomycin is an intercalator antibiotic. An equally important question to ask is whether the aclacinomycin itself changes its conformation in going from the free form to the bound form. The conformation of free aclacinomycin B in D_2O was analyzed using the 2D NOESY data (Figure 8), which showed surprisingly abundant NOE crosspeaks despite the small size of the drug (MW = 809). We note that all NOE crosspeak intensities are consistent with the conformation of AclaB found in the 2:1 complex.

It should be pointed out that the NOE crosspeaks between the protons that are on two ends of a glycosidic linkage define the relative orientation between the two participating moieties. For example, the AKN-H^7 proton has a very strong NOE crosspeak to RN-$H^{1'}$ but has weak NOE crosspeaks to RN-$H^{2'}$/$H^{2''}$, suggesting that the atoms of (AKN)H^7, (AKN)C^7, (AKN)O^7, (RN)$C^{1'}$, and (RN)$H^{1'}$ are nearly coplanar (Figure 8, peak a). Likewise, the NOE crosspeaks between RN-$H^{4'}$ and dF-$H^{1'}$ (peak b) and RN-$HM^{5'}$ and dF-$H^{1'}$ (peak d) are very strong; thus the rhodosamine and deoxyfucose are oriented in such a manner that those two protons are pointing toward

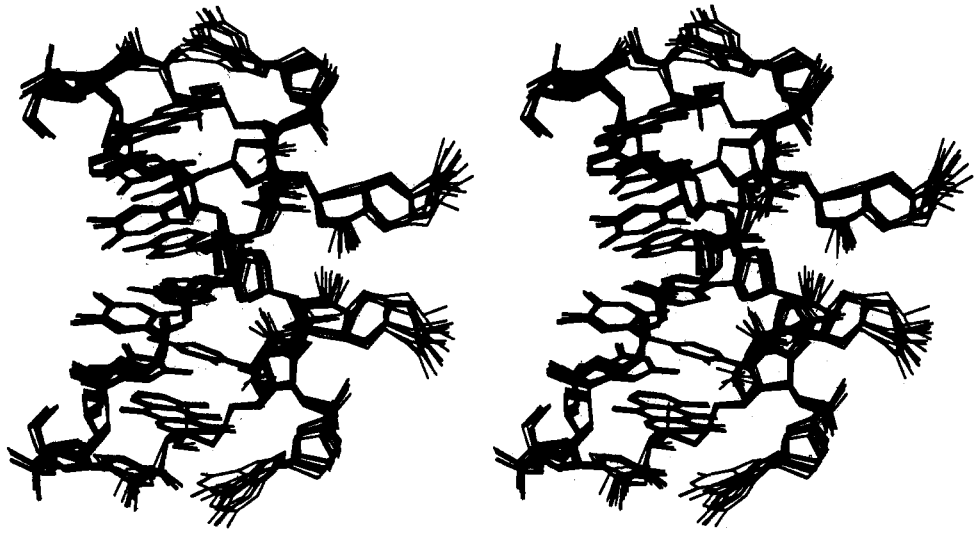

FIGURE 6: Ensemble of 10 refined structures of the 2:1 complex of aclacinomycin B with d(CGTACG) using SPEDREF procedure (incorporating simulated annealing).

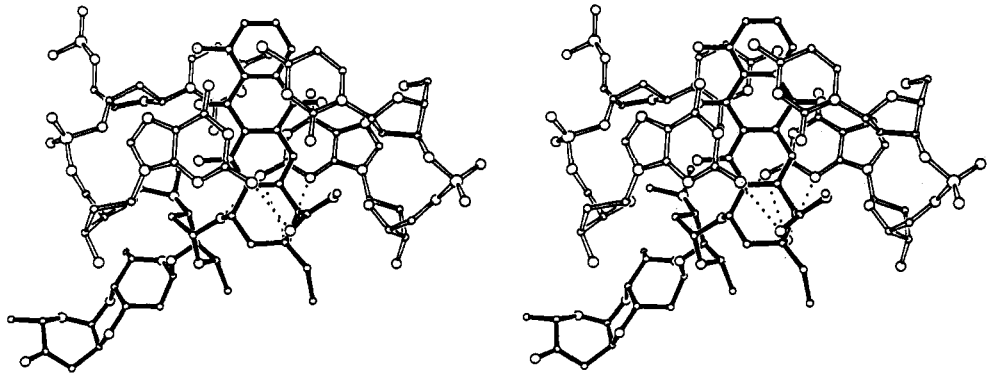

FIGURE 7: View looking perpendicular to the alkavinone of the aclacinomycin B and d(CGTACG) complex, showing the local surroundings of the intercalated drug plus two base pairs (C1pG2 and C5pG6) of the hexamer helix. Four hydrogen bonds between the drug and DNA are shown with dotted lines.

each other. The fused tricyclic ring dF–CinB system has a conformation similar to that found in the crystal structure (Richle et al., 1972), since the expected strong NOE between the dF–$H^{4'}$ and CinB-$H^{5'}$ protons arising from the rigid structure of the ring system is clearly detected (Figure 8, peak c).

From those data we conclude that the conformation of free aclacinomycin B is similar to that of the bound form, at least qualitatively. This observation of a rigid saccharide conformation seems to be quite common, as revealed in the structures of several oligosaccharide antibiotics, including chromomycin A_3 (Silva & Kahne, 1993; Gao et al., 1992) and calicheamicin γ (Walker et al., 1993).

Dynamics of Aclacinomycin Binding. The resonances in the NMR spectra of both 2:1 AclaA–CGTACG and AclaB–CGTACG complexes are broad, with their line widths in the range of ~15–20 Hz at 25 °C (Figure 2). In comparison, the line width of the resonances of free DNA duplex is about 5 Hz at 20 °C. Interestingly, the line width of the resonances of the 0.5:1 and 1:1 complexes is significantly sharper (10–12 Hz) than those of the 2:1 complex. We correlate this observation of variable line widths with the dynamics of the drug binding to DNA.

The binding of aclacinomycin to DNA double helix is a somewhat slow process. This is not entirely surprising since, presumably, the double helix has to partially open (premelt) to allow the chromophore to insert itself between the base pairs. When the concentration of the drug molecule is below the ratio of one drug per hexamer duplex, there are three possible binding sites available, i.e., either C1pG2, G2pT3, or T3pA4. If the binding has no sequence preference, one expects that the drug can bind at any of those three sites and the multiple complexes would be in equilibrium, resulting in an NMR spectrum that is either highly complicated or very broad, or both.

The 1D NMR spectra of the solution containing the 0.5:1 and 1:1 mixtures of AclaA and CGTACG complex show more resonances than those of the 2:1 complex (Figure 2). This is likely the result of a mixture of varying population of the three molecular species (free DNA, 1:1 complex and 2:1 complex), based on the observation that the spectrum is nearly a direct superposition of the spectra of the three species. For example, the resonance at ~8.2 ppm (from $G2H^8$ and $A4H^8$) started to appear in the spectrum of the 0.5:1 complex and grew larger in size in the spectrum of the 1:1 complex. The C^{21} methyl resonance of the bound AclaA had a similar behavior. The similarity of the respective chemical shift of the T-methyl and the $A4H^8$ resonances in the free DNA, 0.5:1, and 1:1 mixtures suggests that the T–A base pair is not perturbed by the intercalation. Therefore, we conclude that the preferred intercalation site of aclacinomycin is CpG. Further support comes from the 2D NOESY spectrum of the 1:1 AclaA–CGTACG mixture at 30 °C, which showed numerous exchange peaks (data not shown). Such an example

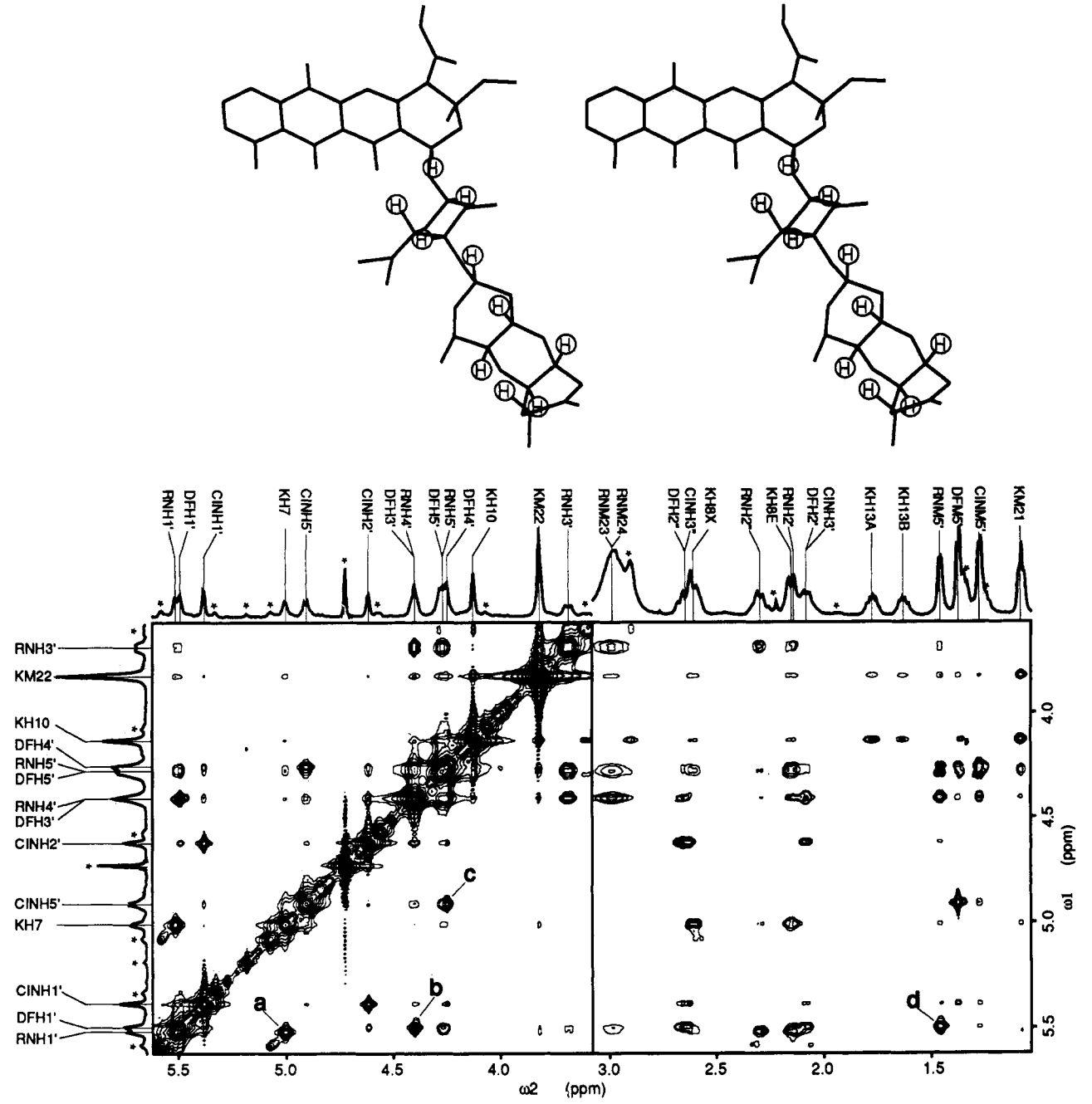

FIGURE 8: Expanded regions of the experimental 2D-NOESY spectrum of aclacinomycin B in D_2O (2 mM concentration). Some key distances between different parts of the molecules are marked. Specifically, those associated with the strong crosspeaks of (a) (AKN)H^7–(RN)$H^{1'}$, (b) (RN)$H^{4'}$–(dF)$H^{1'}$, (c) (dF)$H^{4'}$–(Cin B) $H^{5'}$, and (d) (RN)$Me^{5'}$–(dF)$H^{1'}$ are particularly evident. The structure of the aclacinomycin B in the refined 2:1 complex is depicted.

was also observed in the 1:1 mixture of nogalamycin–CGTACG complex (Robinson et al., 1990).

However, there are some changes in the chemical shifts in going from the free species to the 1:1 complex and finally to the 2:1 complex, indicating that the rate of the exchange between different species is not extremely slow, as compared to that of the nogalamycin (Robinson et al., 1990; Zhang & Patel, 1990; Searle & Bicknell, 1992) or echinomycin (Gilbert et al., 1989). In the case of nogalmycin, its solution of 1:1 mixture contains an almost exact distribution of 25%:50%:25% of free DNA, 1:1 complex, and 2:1 complex, respectively. In the case of echinomycin, the solution of the mixture of echinomycin–CGTACG contained 50%:50% of free and 2:1 complex only, but no 1:1 complex. This is the result of the cooperative interactions between the two echinomycin binding sites, likely due to the formation of the Hoogsteen A–T base pairs (Wang et al., 1984).

The situation in the aclacinomycin complex is opposite to the echinomycin case, i.e., the two adjacent binding sites are slightly antagonistic against each other. When two AclaB molecules bind simultaneously to the hexamer DNA duplex, the two trisaccharide tails, pushing against the sugar–phosphate backbones, possibly destabilize the structure due to their crowding interactions in the minor groove. There may be an exchange between the free and the bound aclacinomycin whose rate is sufficiently slow to allow the exchange crosspeaks to be detected. Indeed, there are several exchange NOE crosspeaks visible in the 2D NOESY spectrum (Figure 2S), likely from the slightly excess drug concentration.

The motion of the complex was further investigated by the studies of the inversion T_1 recovery relaxation time (Figure 4S). It can be seen that the DNA molecule has a longer average T_1 of 1.8 s, whereas the drug molecule is smaller, in the range of 1.2 s, except for the protons (H^1, H^2, and H^3) on ring D of AKN.

CONCLUSION

We have obtained the solution structure of the 2:1 complex by the refinement procedure SPEDREF incorporating simulated annealing (Robinson & Wang, 1992). The results suggested that a CpG step is the preferred binding site for aclacinomycin. However, this remains tentative and should await the results from more careful analysis of drug–DNA complexes involving several DNA sequences or footprinting experiments. The structural perturbation on DNA by aclacinomycin A/B is different from that by daunorubicin/doxorubicin in two respects. First, the entire aclacinomycin covers four base pairs, and the more extensive trisaccharide sugar moiety is projecting further into the solvent region than the daunosamine of daunorubicin/doxorubicin. The complex is more hydrophobic. Second, the kink (caused by AclaA/AclaB) in the DNA double helix near the intercalation site is not seen in the daunorubicin/doxorubicin–DNA complexes. Such structural distortion may be recognized in a unique way by relevant enzymes such as topoisomerase II. Those data suggest that aclacinomycin may have a different biological consequence from that of daunorubicin/doxorubicin in cells.

ACKNOWLEDGMENT

We thank Dr. H. Robinson, Mr. Y. Guan, and Mr. Y. Gao for assistance.

SUPPLEMENTARY MATERIAL AVAILABLE

Four figures (Figures 1S–4S) showing the temperature-dependent 1D NMR spectra, complete 2D NOESY spectra, residual *R*-factors of spins, and inversion recovery relaxation time and one table (Table S1) listing the DNA backbone torsion angles and helical parameters (6 pages). Ordering information is given on any current masthead page.

REFERENCES

Brunger, A. (1992) *X-PLOR*, Version 3.0, The Howard Hughes Medical Institute and Yale University, New Haven, CT.
Chaires, J. B., Fox, K. R., Herrera, J. E., Britt, M., & Waring, M. J. (1987) *Biochemistry 26*, 8227–8236.
Crooke, S. T., & Reich, S. D., Eds. (1980) In *Anthracyclines*, Academic Press, New York.
Denny, W. A. (1989) *Anti-Cancer Drug Des. 4*, 241–263.
Dickerson, R. E., Bansal, M., Calladine, C. R., Diekman, S., Hunter, W. N., Kennard, O., von Kitzing, E., Lavery, R., Nelson, H. C. M., Olson, W. K., Saenger, W., Shakked, Z., Sklenar, H., Soumpasis, D. M., Tung, C.-S., Wang, A. H.-J., & Zhurkin, V. B. (1989) *Nucleic Acids Res. 15*, 247–265.
DuVerney, V. H., Pachter, J. A., & Crooke, S. T. (1979) *Biochemistry 18*, 4024–4030.
Fox, K. R., & Alam, Z. (1992) *Eur J. Biochem. 209*, 31–36.
Gao, Y. G., Liaw, Y. C., Robinson, H., & Wang, A. H.-J. (1990) *Biochemistry 29*, 10307–10316.
Gao, Y.-G., Liaw, Y.-C., Li, Y.-K., van der Marel, G. A., van Boom, J. H., & Wang, A. H.-J. (1991) *Proc. Natl. Acad. Sci. U.S.A. 88*, 4845–4849.
Gao, X., Mirau, P., & Patel, D. (1992) *J. Mol. Biol. 223*, 259–279.
Gilbert, D., & Feigon, J. (1991) *Curr. Opin. Struct. Biol. 1*, 439–445.
Gilbert, D., van der Marel, G. A., van Boom, J. H., & Feigon, J. (1989) *Proc. Natl. Acad. Sci. U.S.A. 86*, 3006–3010.
Jensen, P. B., Jensen, P. S., Demant, E. E. J., Friche, E., Sorensen, B. S., Sehested, M., Wasserman, K., Vindelov, L., Westergaard, O., & Hansen, H. H. (1991) *Cancer Res. 51*, 5093–5099.
Leonard, G. A., Hambley, T. W., McAuley-Hecht, K., Brown, T., & Hunter, W. N. (1993) *Acta Crystallogr. D49*, 458–467.
Liaw, Y. C., Gao, Y. G., Robinson, H., van der Marel, G. A., van Boom, J. H., & Wang, A. H.-J. (1989) *Biochemistry 28*, 9913–9918.
Lown, J. W., Ed. (1988) in *Anthracycline and Anthacenedione-based Anticancer Agents*, Elsevier, New York.
Millot, J.-M., Rasoanaivo, T. D., Morjani, H., & Manfait, M. (1989) *Br. J. Cancer 60*, 678–684.
Oki, T., Takeuchi, T., Oka, S., & Umezawa, H. (1981) *Recent Results Cancer Res. 76*, 21–40.
Richle, W., Winkler, E. K., Hawley, D. M., Dobler, M., & Keller-Schierlein, W. (1972) *Helv. Chim. Acta 55*, 467–480.
Robinson, H., & Wang, A. H.-J. (1992) *Biochemistry 31*, 3524–3533.
Robinson, H., Liaw, Y. C., van der Marel, G. A., van Boom, J. H., & Wang, A. H.-J. (1990) *Nucleic Acids Res. 18*, 4851–4858.
Searle, M., & Bicknell, W. (1992) *Eur. J. Biochem. 205*, 45–58.
Silva, D. J., & Kahne, D. E. (1993) *J. Am. Chem. Soc. 115*, 7962–7970.
Sriram, M., Liaw, Y.-C., Gao, Y.-G., & Wang, A. H.-J. (1991) *J. Biomol. Struct. Dyn. 9*, 251–269.
Tapiero, H., Boule, D., Trincal, G., Fourcade, A., & Lampidis, T. J. (1988) *Leuk. Res. 12*, 411–418.
Walker, S., Murnick, J., & Kahne, D. E. (1993) *J. Am. Chem. Soc. 115*, 7950–7961.
Wang, A. H.-J. (1992) *Curr. Opin. Struct. Biol. 2*, 361–368.
Wang, A. H.-J., Ughetto, G., Quigley, G. J., Hakoshima, T., van der Marel, G. A., van Boom, J. H., & Rich, A. (1984) *Science 225*, 1115–1121.
Wang, A. H.-J., Ughetto, G., Quigley, G. J., & Rich, A. (1987) *Biochemistry 26*, 1152–1163.
Williams, L. D., Egli, M., Gao, Q., Bash, P., van der Marel, G. A., van Boom, J. H., Rich, A., & Frederick, C. A. (1990) *Proc. Natl. Acad. Sci. U.S.A. 87*, 2225–2229.
Yoshimoto, A., Johdo, O., Watanabe, Y., Nishida, H., & Okamoto, R. (1992) *J. Antibiot. 45*, 1005–1007.
Zhang, X., & Patel, D. J. (1990) *Biochemistry 29*, 9451–9466.
Zhang, H., Gao, Y.-G., van der Marel, G. A., van Boom, J. H., & Wang, A. H.-J. (1993) *J. Biol. Chem. 268*, 10095–10101.